mSystems Submission Template mSystems Submission Template mSystems Submission Template mSystems Submission Template mSystems Submission Template mSystems Submission Template

RESEARCH ARTICLE

Mechanisms of *Listeria monocytogenes* disinfection with Benzalkonium chloride: from molecular dynamics to kinetics of time-kill curves

Martín Pérez-Rodríguez,[a,c] Marta L. Cabo,[b] Eva Balsa-Canto,[a] Míriam R. García[a,*]
[a]Biosystems and Bioprocess Engineering Group, IIM-CSIC Spanish National Research Council, Vigo, Spain
[b]Microbiology Group, IIM-CSIC Spanish National Research Council, Vigo, Spain
[c]Present affiliation: Applied Physics Department, Faculty of Science, University of Vigo, Vigo, Spain

Compiled June 16, 2022
This is a draft manuscript, pre-submission

Address correspondence to Míriam R. García, miriamr@iim.csic.es.

ABSTRACT Unravelling the mechanisms of action of disinfectants is essential to optimize dosing regimes and minimize the emergence of antimicrobial resistance. In this work, we decipher the mechanisms of action of a commonly used disinfectant - benzalkonium chloride (BAC)- over a major pathogen -*L. monocytogenes*- in the food industry. For that purpose, we use modeling at multiple scales, from the cell membrane to the cell population inactivation. Molecular modeling reveals that the integration of the BAC into the membrane requires three phases: (1) the BAC approaches the cellular membrane, (2) the BAC is adsorbed on its surface, and (2) it is rapidly integrated into the lipid bilayer, where it remains at least for several nanoseconds, probably destabilizing the membrane. We hypothesize that the equilibrium of adsorption, although fast, is limiting for sufficiently large BAC concentrations, and a kinetic model is derived to describe kill curves of a large population of cells. The model is tested and validated with time series data of free BAC decay and time-kill curves of *L. monocytogenes* at different inocula and BAC dose concentrations. The knowledge gained from the molecular simulation plus the proposed kinetic model offers the means to rationally design novel disinfection processes.

IMPORTANCE Disinfection is fundamental to guarantee food safety, but the misuse or overuse of common biocides in the food industry, such as benzalkonium chloride, can act as drivers of antimicrobial resistance. Selective pressure associated with exposure to benzalkonium chloride may result in adaptation to quaternary amine compounds or even cross-resistance to other antibiotics such as ciprofloxacin. Therefore, understanding the mechanisms of action of disinfectants is crucial to determining the optimal dosing regimens to ensure safety while minimizing the levels of disinfectant residue after treatment.

KEYWORDS: *Listeria monocytogenes*, Benzalkonium Chloride (BAC), Mechanisms of Disinfection, Molecular Dynamics, Membrane Adsorption, Predictive Microbiology

INTRODUCTION

Benzalkonium chloride (BAC) is one of the usual active compounds in disinfectants (1), despite its potential to promote antimicrobial resistance, for example, the survival of persistent tolerant subpopulations of *E. coli* during multiple periodic disinfection (2). Moreover, BAC is chemically very stable and might persist in the environment for

months, promoting resistance against quaternary ammonium compounds (QACs) or even cross-resistance to antibiotics. Taking into account the wide use of BAC (in domestic, agricultural, industrial and clinical applications) and its increasing overuse in recent years during the coronavirus disease pandemic (3), understanding the mechanisms of action is of great relevance to allow a more rational use of this widely applied disinfectant.

Listeria monocytogenes is one of the most relevant and ubiquitous pathogens in the food industry and is being disinfected with BAC. According to the latest One Health Report published by the European Food Safety Authority, listeriosis has the highest proportion of hospitalizations of EU zoonoses, with a final mortality of 14% (4) *Listeria monocytogenes* can survive throughout the food chain, from the environment to food products and can persist for long periods of time adhered to the surfaces of food industrial settings, normally associated with other bacterial species that form part of biofilms (5).

It has been extensively reported that *L. monocytogenes* can easily develop adaptation when exposed to sublethal concentrations of BAC (6, 7, 8) and even cross-adaptation to antibiotics (9, 10). The molecular and physiological mechanisms of BAC adaptation are not fully known, although most authors have related several BAC efflux pump systems, located on the chromosome (mdrL) and associated with mobile genetic elements (qacH, brcABC, edrm) (11). Nevertheless, no effect of efflux pump inhibitors (with reserpine) is observed in resistant strains adapted to BAC (12, 9). Therefore, alternative mechanisms are proposed, such as modification of the cell wall (13, 12), decreased uptake, biofilm formation, or entry into the viable but not culturable state (14). Therefore, any progress in unraveling the mechanism of action of BAC would contribute to overcoming the resistance problem to BAC in *L. monocytogenes*.

Molecular dynamics are the theoretical tool to decipher the mechanisms of action of biocides when entering cellular membranes, as already proposed and studied for the interaction of QACs with membranes of *E coli* and *Staphylococcus aureus* Alkhalifa et al. (15). The hypothesis proposed in this work, after simulations showing that QACs approach the negatively charged membrane and are later integrated into the lipid bilayer, describes that the electrically charged membrane is a prerequisite for binding and the hydrophobic interaction lipid-QAC drives the integration of the QACs into the membrane. However, these molecular mechanisms have not yet been tested to understand the kinetics of disinfection of QACs for populations of pathogenic bacteria.

In this work, our aim is to understand the mechanisms by which BAC inactivates *L. monocytogenes* and to predict the dynamics of inactivation at the population level. First, we simulate the behavior of a molecule of BAC close to a membrane with a standard composition of *L. monocytogenes* using molecular dynamics. Second, the results of the simulation are used to derive the assumptions required for a kinetic model of the inactivation of bacteria with BAC. The model was finally calibrated and experimentally validated.

RESULTS

Insight from Molecular dynamics: Integration of BAC into the *L. monocytogenes* membrane Simulations of molecular dynamics show that BAC is integrated into the membrane of the *L. monocytogenes* very fast, in less than 20 ns in all simulations. Integration proceeded in three phases, as illustrated in figure 1. Firstly, BAC moves randomly, is later adsorbed by the membrane surface, and is then integrated into the membrane. The dynamic behavior after integration is similar to the molecules of the lipid membrane, as was observed by extending the simulation times to 40 ns in total.

mSystems Submission Template mSystems Submission Template mSystems Submission Template mSystems Submission Template mSystems Submission Template mSystems Submission Template

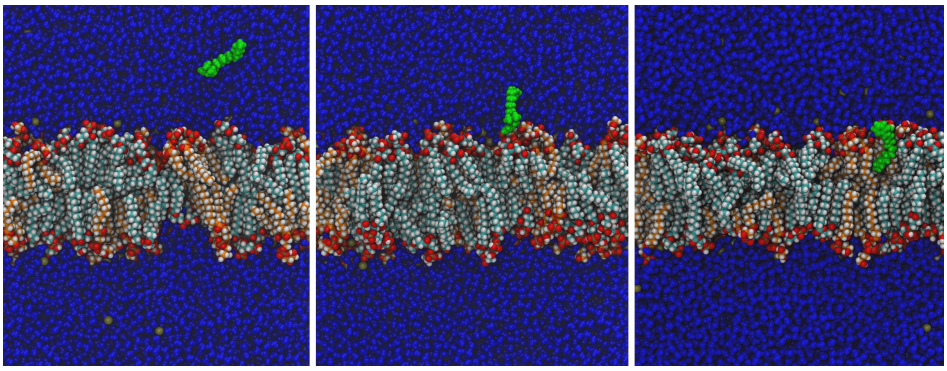

FIG 1 Molecular dynamics simulation of BAC integration into the cell membrane. When a BAC molecule is placed in the vicinity of the bacterial membrane (left frame), it is attracted and attached to the surface (center frame). Eventually, the molecule is completely integrated (right frame). All BAC atoms are drawn in green color, and water is drawn in dark blue. Lipids are colored by atom type, alkyl chains of CL are colored light blue, and PG are colored orange. The dark yellow spheres in water correspond to K+ counterions. These three snapshots were taken at 3 ns (left), 5 ns (center), and 8 ns (right) form one of the simulations at 37ºC whith BAC starting at 11 nm from origin of coordinates, after usual equilibration of water-membrane system. Sections are perpendicular to the plane of the membrane. For the sake of clarity, only molecules behind the BAC center of mass are represented.

To analyze in more detail the integration process, the trajectory of the N atom and C12 at the end of the BAC tail was extracted from each simulation, and its z coordinate was represented with respect to time, as in Figure 2. Here, only one particular simulation is represented for better clarity, but six simulations were calculated to estimate the statistics for the different times. Three regions are easily distinguishable, chronologically corresponding to the phases of (1) approaching, (2) adsorption, and (3) membrane integration. First, the selected C12 atom moves randomly around the start position with the molecule over the membrane surface until the N atom is attached to the membrane, marking the beginning of the adsorbed phase. After 8±6 ns, water repulsion drives the C tail inside the hydrophobic region, which ends aligned with the rest of the lipids. This integration phase lasts 4±1 ns.

The short time obtained from simulations for the three phases, combined with the seamless integration of BAC, and the stability of the membrane afterwards, implies a very high affinity of BAC for the membrane. Moreover, it is arguable that BAC will not abandon the membrane once it is integrated. These results support the hypothesis in the present work that BAC may be significantly trapped by bacteria, in a nonreversible way, and may even remain integrated into the membrane long after cellular lysis.

Modelling population kinetics of time-kill curves based on insight from molecular dynamics Molecular dynamics provides information to elucidate the main mechanism by which BAC is expected to kill populations of *L. monocytogenes* and probably other bacteria with a similar membrane composition. The main assumption is that cells die when a sufficient concentration of BAC is integrated into the membrane using the rational model, common in chemical disinfection (16):

$$\frac{dN}{dt} = -k_d N^x C^n$$

where N is the bacterial concentration at any time, k_d is the constant of the inactivation rate, n the concentration of dilution and x the constant describing the behavior of shoulders ($x < 1$) or tailing ($x > 1$) behavior. However, instead of directly using the

mSystems Submission Template mSystems Submission Template mSystems Submission Template mSystems Submission Template mSystems Submission Template mSystems Submission Template

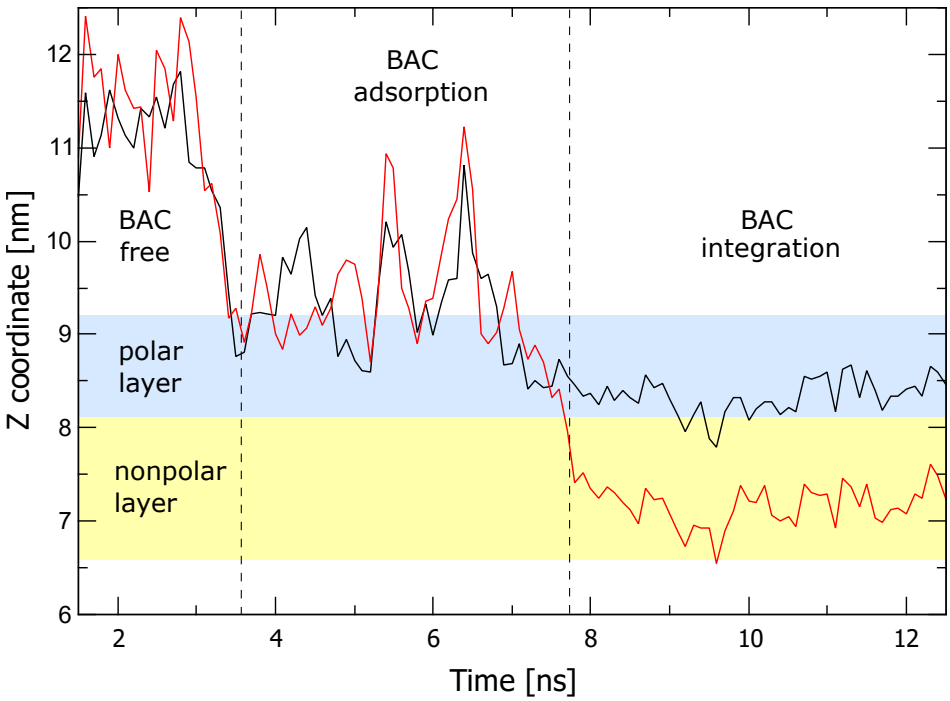

FIG 2 Evolution with time of z coordinate of the N atom (black) and the C12 atom (red) of BAC, extracted from one of the simulations starting at z = 11 nm. The approximate region occupied by the membrane upper leaflet is highlighted for reference, divided into polar layer (blue) and nonpolar layer (yellow). z values of the N and C12 atoms move in parallel until BAC is integrated, after which N remains in the polar layer of the membrane, but C12 migrates to the bottom of the nonpolar layer. Compare with 1.

disinfectant dose, we make the kill curve dependent on the disinfectant concentration on the membrane C_m following a Hill function, a common model in pharmacokinetic and pharmacodynamic (17) and previously used to describe other QAC disinfection dynamics (18). Therefore, the model reads:

$$\frac{dN}{dt} = -k_d N^x \frac{C_m^n}{C_m^n + k_m^n}$$

where k_m is the half maximal effective concentration (disinfectant concentrations at which 50% of the maximum effect is obtained) and n is the Hill coefficient shaping the effect of the disinfectant (higher values model sharp functions, similar to step functions with only two possible values, and low values simulates a sigmoid curve). We assume that the cell dies once the concentration of disinfectant in the cell membrane exceeds a certain threshold value k_m. Therefore, the Hill function is sharp and the coefficient high enough to be fixed at $n = 30$. Note that the cell is alive, while the BAC in the membrane is less than k_m, and this concentration is kind of a minimum inhibitory concentration (MIC), but measured over the disinfectant concentration in the membrane, instead of considering the added BAC.

For modeling the disinfectant concentration on the membrane C_m, we assume the following:

- The total amount of BAC added at the initial time m_0 goes to adsorbed BAC on different surfaces (m_s), on the cell membrane (m_m) or is free in the medium (m_f). Therefore, the total amount of BAC in the membrane, using a mass balance equation, is the following:

$$m_m = m_0 - m_s - m_f$$

mSystems Submission Template mSystems Submission Template mSystems Submission Template mSystems Submission Template mSystems Submission Template mSystems Submission Template

- Adsorbed BAC on other surfaces (m_s), such as glass vessels or polystyrene well plates, is a very fast process and, therefore, for the time scale considered, m_s should saturate to a constant concentration very quickly. In other words, we assume that this process is faster than BAC membrane integration and that dynamics should not be included in the model. This is supported by the experiments in (19), showing also that the percentage of Adsorbed BAC in glassware is especially relevant for low concentrations of BAC added.
- BAC in the membrane (m_m) is assumed to be limited by the adsorption phase when there is excess BAC. Implicitly, we assume that any adsorbed BAC is later integrated into the membrane, causing membrane destabilization when the membrane concentration C_m is sufficiently high as described for the rational model. To relate the concentration and mass of adsorbed BAC, we need the total surface of the cellular membrane, which we assume is the surface of one cell S_{cell} multiplied by the number of initial cells or inocula (N_0), therefore, the mass balance now reads as follows:

$$C_m\, S_{cell}\, N_0 = m_0 - m_s - m_f.$$

  Note that the mass balance provides a link to explain the BAC dosage in different inocula or the so-called "inoculum effect", observed for BAC and *E. coli* (20).
- Adsorption is also sufficiently fast, predicted to be around 3 nanoseconds by molecular dynamics, as shown in Figure 2, to assume that the dynamics of adsorption rapidly reach equilibrium and are not required to be modeled for the time scales of the experiment. Therefore, the concentration in the membrane C_m is in equilibrium with the free disinfectant C_f following a linear adsorption isotherm $C_m = K_H\, C_f$. Note that the mass and concentration of free BAC are equivalent since experiments were carried out for a volume of 1ml ($m_f\, 1 = C_f$), same for the initial mass and concentration of BAC ($m_0\, 1 = C_0$). Therefore, by combining the adsorption isotherm with the mass balance, we derive the BAC concentration in the membrane as a function of the membrane surface $S_{cell}\, N_0$, Henry's constant K_H and BAC mass added and in surface

$$C_m = \frac{C_0 - m_s}{S_{cell}\, N_0 + (1/K_H)}.$$

We further assume a value of $S_{cell} = 3.52e-8cm^2$ based on a capsule surface of *L monocytogenes* with radius $0.335\mu m$ (half the width in (21)) and length 1 ($2.5\mu m$ in (21) including the caps of the capsule). Note that this diameter changes from division to division and that even the effective membrane of adsorption may differ, owing to a different membrane composition, from the real membrane surface. However, this parameter cannot be estimated from population concentrations (the parameters are not structurally identifiable (22)) and must be fixed to some realistic value.

Under these assumptions, the model finally reads as follows:

$$\frac{dN}{dt} = -k_d N^x \frac{C_m^n}{C_m^n + k_m^n} \tag{1a}$$

with

$$C_m = \frac{C_0 - m_s}{S_{cell} N_0 + (1/K_H)} \tag{1b}$$

$$C_f = (1/K_H) C_m. \tag{1c}$$

The table 1 describes the meaning and information of the different parameters and variables of the model.

mSystems Submission Template mSystems Submission Template mSystems Submission Template mSystems Submission Template mSystems Submission Template mSystems Submission Template

TABLE 1 Variables and parameters of the model. The variables are always calculated by the model, and some are compared to measured data to estimate unknown parameters. Parameters are assigned based on the experimental design (inoculum and BAC dose), estimated by fitting to experimental data, or assumed when information is available.

Variables		
N	*Listeria* concentration	Calculated and measured $[CFU/ml]$
C_f	Free BAC	Calculated and measured $[ppm = \mu g/mL]$
C_m	BAC in cell membrane	Calculated $[\mu g/cm^2]$
Parameters		
C_0	BAC initial concentration (dose)	Defined by the experimental design $[ppm]$
N_0	Inoculum *Listeria*	Defined by the experimental design $[CFU/ml]$
n	Hill constant	Assumed 30$[-]$
S_{cell}	Cell Membrane surface	Assumed $3.52 \times 10^{-8}[cm^2]$
x	Constant Rational model	Estimated 1.40$[-]$
k_d	Inactivation rate constant	Estimated 0.23$[min^{-1}(CFU/ml)^{1/x}]$
k_m	Adsorbed BAC to kill the cell	Estimated 2.02$[\mu g/cm^2]$
K_H	Henry's isotherm constant	Estimated 0.17$[cm^{-1}]$
m_s	Adsorbed BAC on surfaces	Calculated 20.42$[\mu g]$

Calibration with Validation The model and its underlying hypothesis are tested using experimental data. Other alternative models, based on different assumptions or in previous models, such as the semi-empirical model in (20), were also tested until the final model in this work was obtained.

Two steps were required for the testing. First, we estimated the unknown parameters confronting the model with data from four experiments with two different levels of inoculum and BAC dosage and their respective combination, following the log-likelihood method described in the methods section. The final model prediction is compared with a new experiment that was not used for the estimation for different inoculum and BAC dosage conditions. This experiment, named the validation experiment, helps us assess the ability of the model to predict behaviors different from those originally used for estimation.

Figure 3 shows the goodness of fit for the experiments used for the estimation ($\approx$ 8 and 10 logs of inoculum at 40 and 50 ppm) and for validation ($\approx$ 6 logs of inoculum and 60ppm). As expected, the goodness of fit is better for the estimation experiments than for the validation. Nevertheless, considering that the validation is an extrapolation where the initial condition is not within the range of the estimated experiments), performance is significantly good, especially for BAC with less variability in the measured data.

DISCUSSION

The mechanisms of action of QACs have been postulated in the literature as a chain of events where interactions of QACs with the bacterial membrane remain the first and therefore necessary step. In the 1960s, Salton (23) proposed a possible sequence of events that starts with (1) adsorption and penetration of the agent into the cell wall,

mSystems Submission Template mSystems Submission Template mSystems Submission Template mSystems Submission Template mSystems Submission Template mSystems Submission Template

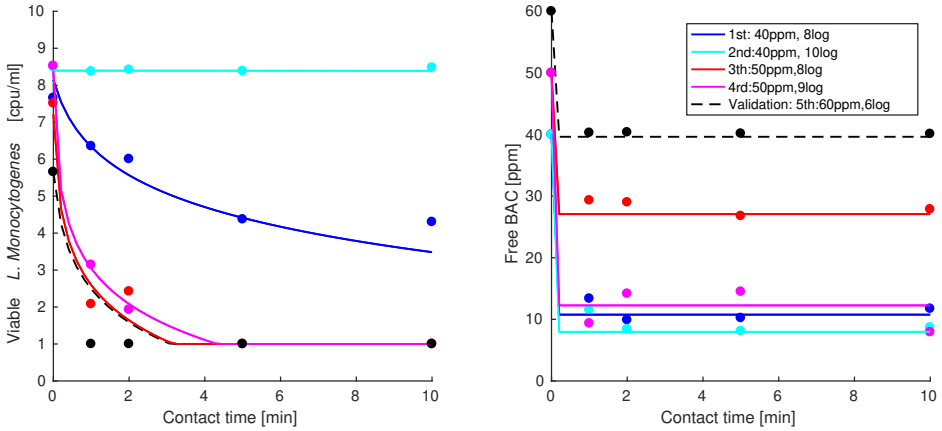

FIG 3 Fit (Experiments 1-4) and validation (Experiment 5). Based on experimental replicas, 2.5 std is assumed for B and 0.5 for viable counts on the log scale for the maximum log-likelihood estimation problem.

(2) reaction and disorganization of the cytoplasmic membrane to a later (3) leakage of low molecular weight intracellular material, and (4) degradation of proteins and nucleic acids and (5) wall lysis. Although other main mechanisms of action have been proposed, the membrane continues to be, if not the main, a necessary first target (24, 25, 26, 27, 28, 29). This is supported by the fact that the action of QAC increases when using cell permeabilizing agents (24) and is stronger for Gram-positive bacteria (25).

The simulations of the molecular dynamics in this work (Figure 1-2) describe the first event in Salton's theory with three phases: approach, adsorption, and integration of BAC into the membrane. The molecular dynamics also show that BAC has high affinity for the membrane and a low probability of entering the cell when the membrane structure is intact for only one BAC molecule. Therefore, more than one BAC molecule is needed for the proposed chain of events, until the final leakage, degradation of intracellular molecules, and lysis.

A variety of experimental and computational membrane models can be found in recent reviews (30), some of them related to drug or disinfectant interactions. These include molecular dynamics studies of gram-positive and gram-negative bacteria, especially *E. coli* and to a lesser extent of *P. aeruginosa*. However, to the best of our knowledge, none of them directly models the BAC interaction with the *L. monocytogenes* membrane. Alkhalifa *et. al* simulated the destabilization of the *E. coli* and *S. aureus* model membranes by quaternary ammonium compounds (QAC). Their description of the QAC integration process, in three phases, is in very good accordance with our results, supporting also the application of Salton's theory. Another relevant work for our purposes is that of Zhao *et. al* (31), where, using molecular dynamics, they study the mechanical properties of lipid bilayers made of dioleoyloxytrimethylammonium propane (DOTAP) and dimyristoylphosphatidylcholine (DMPC). The key finding in this work is that the addition of unsaturated DOTAP, an ammonium alkyl amphiphile, promotes lipid chain interdigitation and fluidizes the lipid bilayer. This result agrees with our simulations and suggests that the progressive addition of BAC will correspondingly increase the fluidity of the *L. monocytogenes* membrane. Eventually, the addition of enough amounts of BAC would make the membrane too fluid to support the interfacial tension, compromising membrane functions and integrity and thus leading to leakage and degradation.

mSystems Submission Template mSystems Submission Template mSystems Submission Template mSystems Submission Template mSystems Submission Template mSystems Submission Template

Molecular dynamics, in addition to supporting the first event in Salton's theory, provides the needed insight for the derivation of a kinetic model of population dynamics describing the time-kill curves. The first and most relevant consideration is that fast molecular dynamics should be approximated to be able to derive a kinetic model capable of describing the kill curves at a different time scale and considering a population of bacteria with their membranes. We should stress two major differences between both models: the aim of the modeling (a piece of membrane versus millions of cells with their membranes) and the time scales (less than 20 ns for molecular dynamics versus minutes for time-kill curves).

The population dynamic model that describes the time-kill curves assumes the killing following a rational model function of the BAC membrane in the cell calculated based on the adsorption equilibrium. The first phase of adsorption was fast in the molecular simulations (less than 5 ns, Figure 2) comparing the killing dynamics (minutes 3), and is assumed as an equilibrium based on Henry's isotherm constant (K_H). This isotherm provides a linear relationship between the free measured BAC (C_f) and the BAC concentration in the membrane (C_m). The estimated value for this constant was $0.17[cm^{-1}]$, which means that the BAC membrane concentration is higher than the free BAC concentration, in agreement with the high affinity observed for BAC to bacterial membranes in molecular dynamics simulations.

A interesting estimation of the model is the minimum concentration of integrated BAC required to kill the cell $k_m = 2.02[\mu g/cm^2]$, that is used as a based to give a mechanistic explanation of the inoculum effect (20). This value is obtained using a population model and represents an average value that depends on many factors such as the nutrient medium or the bacterial growth state, but also on the exposed cellular surface. Note that the minimum concentration to kill the cell depends on the adsorption equilibrium and therefore on the adsorption surface, here modelled as the sum of the surfaces of the initial number of cells or inoculum. The resulting expression, equation (1b), provides an explanation of the inoculum effect without complex dynamics or large number of parameters. The inoculum effect is usually ignored for disinfectants, and the models considering this effect in antibiotics require complex dynamics, and therefore more parameters must be estimated than the model proposed here. See, for example, the pharmacokinetic / pharmacodynamic model in (32) for describing the killing curves of *E. coli* with ciprofloxacin. That effect was first detected and modeled in (20) for *E. coli* and BAC, but required an empirical mathematical expression, without any mechanistic insight, which needs to be adapted for each pair of antimicrobial-bacteria. In fact, the tests we conducted to model the killing curves of *L. monocytogenes* with this model were unsatisfactory.

In future work, simulations of molecular dynamics should be further extended to account for more realistic scenarios in which many BAC molecules are adsorbed in Gram-positive bacteria. Note that current simulations with one BAC molecule predict its integration into the membrane with low exit possibilities (very stable state), which confronts the known resistance mechanisms associated with overexpression or acquisition of efflux pumps that affect mainly Gram negative cells, but also Gram positive cells and *L. monocytogenes* (33, 7, 34). It should be stressed that other works have also postulated mechanisms of action of QACs at the membrane level, without these molecules entering the cytoplasm even if at high concentrations (35). Therefore, more theoretical and experimental studies are needed to explain this apparent contradiction between the mechanisms of action focused on the membrane and the resistance mechanisms due to removal of QACs with efflux pumps.

mSystems Submission Template mSystems Submission Template mSystems Submission Template mSystems Submission Template mSystems Submission Template mSystems Submission Template

mSystems Submission Template mSystems Submission Template mSystems Submission Template mSystems Submission Template mSystems Submission Template mSystems Submission Template

CONCLUSIONS

Elucidating the mechanisms of action of Quaternary Ammonium Compounds is critical to optimize disinfection protocols and avoid the adaptation of bacteria to disinfectants or even other antimicrobials, such as antibiotics. Whereas the accepted hypothesis of the 1960s describes a chain of events beginning with the first necessary membrane adsorption of the disinfectant molecule, that event had not yet been modeled for the pair of benzalkonium chloride (BAC) and *L. monocytogenes*. Molecular dynamics simulations show three phases where one BAC molecule (1) approaches, (2) is adsorbed, and (3) is integrated into the bacterial membrane. Inspired by these molecular simulations, we postulate a kinetic model capable of describing time-kill curves of populations of *L. monocytogenes* at different doses of BAC and initial inoculum numbers. The mechanistic model assumes that a cell dies when a sufficiently large number of BAC molecules are integrated into the membrane whose surface depends on the number of initial bacteria, and therefore explains the known "inoculum effect" in chemical disinfection.

MATERIALS AND METHODS

Experimental methods *L. monocytogenes* IIM-L168 was isolated and genetically characterized in a previous survey carried out on pre-sanitized fish processing surfaces (36). Stock cultures were maintained at -80ºC in brain heart infusion broth (BHI; Biolife, Milan, Italy) containing 50% glycerol 1:1. The working cultures were kept at -20ºC in Trypticase Soy Broth (TSB, Cultimed, Barcelona) containing 50% glycerol 1:1 (v/v) as well. 100 (microliters) of the working culture were grown overnight at 37 ° C in 5 ml of TSB and subcultured and incubated overnight under the same conditions to ensure proper growth. *L. monocytogenes* culture was centrifuged (4 min, 8500g, centrifuge: Sigma, 2-16K) and the pellet resuspended in 0.85% (w/v) NaCl. Resuspended cells were adjusted to Abs 700=0.1 in sterile NaCl 0,85% (W / v), which according to previous calibrations correspond approximately to a cell concentration of 10 log CFU/ml. The rest of the concentrations used in the experiments were prepared by serial dilution in NaCl 0.85% (w/v).

Benzalkonium chloride solutions (Sigma-Aldrich) were prepared in sterilized deionized water at the concentrations established in the experimental design (40, 50 and 60 ppm). Dose response series were prepared by adding 1 ml of BAC to sterile tubes containing 1 ml of *L. monocytogenes* inoculum and allowed to act for 1, 2, 5 and 10 min at 25 ° C without shaking. In the control tubes, NaCl 0.% (w/v)was added instead of BAC. After exposure, the culture was divided into two subsamples for subsequent analysis: a) 500 microliters were neutralized by adding the same volume of neutralizing solution (composition per L: 10 ml of a 34 g/l KH2PO4 buffer (pH=7.2); 3g soybean lecitin ; 30 mL Tween 80; 5g Na2S203; 1 g L-histidine) for 10 minutes at room temperature and used to determine the number of viable cultivable cells. The quantification of VCC was carried out by serial diluting, spreading in TSA (Cultimed, Barcelona, Spain) and counting after incubation at 37 ° C for 48 h. The results were expressed in log CFU/ml and b) 1500 microliters were filter sterilized through a 0.2 micrometer syringe filter (Sartorious, Gottingen, Germany) and the filtrate was used to determine the extracytoplasmic BAC concentration following the method described by Scott (1968).

Molecular dynamics We have prepared a model membrane for Molecular Dynamics (MD) simulations using consensus data from two experimental works in the literature (37) and (38). As we are interested in simulating the stationary phase, we have chosen the data at 37ºC, because it is the optimal growing temperature, and the data were collected over more time at this temperature. To achieve a computationally tractable and realistic model, we have made a number of simplifications. First,

we selected only the principal lipids that were properly identified: cardiolipin (CL); lysylcardiolipin (LysCL); phosphatidylglycerol (PG) and lysylphosphatidylglycerol (LysPG). Second, because the Lys moiety in LysCL and LysPG is outside the hydrophobic membrane region, we have just considered that lipids with and without Lys are equivalent for the BAC interactions with the membrane. Therefore, we added relative PG concentrations in (38) obtaining a 59 % that is compatible with the 70 % mentioned in (37), taking into account the variability with time of the lipid composition and the uncertainty of this type of data. Furthermore, considering the length of alkyl chains in commercial BAC, we made the additional simplification of choosing all 14 lipid alkyl chains (for example, BAC 12060, Sigma Aldrich, contains 70% benzyldimethyldodecylammonium chloride and 30 % benzyldimethyltetradecylammonium chloride, approximately). All this resulted in a membrane model with a composition of 70 % PG-14 and 30 % CL-14.

Simulations were setup on laboratory computers and then completed at CESGA (Supercomputer Center of Galicia), using GROMACS (39) with the CHARMM36 force field. The initial structures and parameters were obtained with the help of a CHARMM-GUI input generator (40). CHARMM-GUI (41) is an online facility that runs CHARMM (42) in the background and provides a collection of convenient tools for setting up different types of systems, particularly lipid membranes (43) and new ligands (44) among them. We have used VMD (45) for the visualization of structures and the rendering of figures.

We started building a bilayer of 105 molecules of PG and 45 molecules of CL per leaflet, randomly distributed, with identical relative concentrations in both leaflets. This bilayer was neutralized with K + cations and dissolved with a column of water (TIP3P) up to 5 nm over each leaflet to ensure that the free movement of BAC around the lipids is allowed. The resulting box is then an approximate cube of 10 x 10 x 13 nm containing 38261 molecules of water surrounding a bilayer of 300 lipids. After a first equilibration of this box, one molecule of BAC was added, and then the system was reequilibrated, following several progressively less restrictive steps. BAC molecule was inserted in 3 different places: near the membrane surface, at the top end of the water column, and at an intermediate place between them. In particular, in the middle of the box in the (x,y) plane and with z coordinates of 10, 11, and 13 nm (at a distance of 1.5, 2.5, and 4.5 nm from the membrane surface). The resultant 3 instances were run independently, in two replicas each one. The replica of each simulation instance produced a trajectory almost identical to the original, as expected for well-equilibrated systems. Simulations were first tested at 30º C to match the usual room temperature and then repeated at 37º C, the optimal growing temperature *L. monocytogenes*.

After reequilibration, restriction-free NPT production was performed in each instance, using the Nose-Hover thermostat (46) and the Parrinello-Rahman barostat (47) with standard compressibility, in semiisotropic mode to isolate pressure in the dimensions of the membrane plane (x, y) from the perpendicular dimension (z). Simulations were carried out until the BAC was fully integrated into the leaflet structure. After that, they were extended at least another 20 ns to assess the stability of BAC integration into the membrane. Stability was confirmed by monitoring the energy and mechanical behavior of the systems.

Kinetic modeling based on BAC adsorption The kinetic model derived in this work describes the dynamics of *L. Monocytogenes* kill curves and levels of BAC residues (free BAC outside the cell) at different dose concentrations of inocula and BAC. The model is deterministic and has validity above 100 CFUs/ml. Any value (simulated or measured) below this limit has great variability and will be considered ≤ 100, without specifying any number (20).

We need numerical methods to simulate the model, estimate unknown param-

mSystems Submission Template mSystems Submission Template mSystems Submission Template mSystems Submission Template mSystems Submission Template mSystems Submission Template

mSystems Submission Template mSystems Submission Template mSystems Submission Template mSystems Submission Template mSystems Submission Template mSystems Submission Template

eters from available experimental data, and analyze the calibration results. In this work, we use AMIGO2 software (Advanced Model Identification using Global Optimization) for simulation and parameter estimation. This is a multi-platform toolbox implemented in Matlab (48).

Parameter estimation is based on maximization of the log-likelihood function. The idea is to find the parameter vector that gives the highest likelihood to the measured data (49). For independent measurements with Gaussian noise, the problem becomes minimizing the minimum square error weighted with the standard deviations associated with each measurement:

$$J = \sum_{i=1}^{n} \frac{(\log 10(N_i) - \log 10(\hat{N}_i))^2}{\sigma_N^2} + \sum_{i=1}^{n} \frac{(C_i - \hat{C}_i)^2}{\sigma_C^2}$$

where N_i and C_i are the time measurements for *L. monocytogenes* and BAC and $\hat{N}_i$ and $\hat{C}_i$ their respective estimations using the model and n is the number of time measurements for all experiments. We consider a logarithmic scale for the viable cells to avoid computational problems derived from the different orders of magnitude. We assume that both standard deviations (σ_N and σ_C) are constants and can be approximated from the replicates of the data, resulting in $\sigma_N = 0.5$ and σ_C=2.5, see (20) for details.

Validation was performed confronting the model predictions with experimental data not used for calibration and obtained for different inocula *L. monocytogenes* and BAC dosing concentrations.

SUPPLEMENTAL MATERIAL

Video S1-S3 Supplemental files the molecular dynamics of three different simulations related to the study.

Modelling codes, including data are provided in https://doi.org/10.5281/zenodo.6651604 (50)

ACKNOWLEDGMENTS

We acknowledge the funding received from the MCIN/AEI/10.13039/501100011033 (grant RTI2018-093560-J-I00, "ERDF A way of making Europe"), from CSIC (grant 20213AT001) and Xunta de Galicia (grant GAIN IN607B 2020/03).

MRG and EBC designed the original idea. MPR and MRG studied and conducted the computational experiments and analysis. MLC designed and conducted the experimental study. All authors have drafted, reviewed the manuscript and agreed to the published version of the manuscript.

REFERENCES

1. **Tezel U, Pavlostathis SG**. 12 2011. Role of Quaternary Ammonium Compounds on Antimicrobial Resistance in the Environment, p 349–387. *In* Antimicrobial Resistance in the Environment. John Wiley & Sons, Inc., Hoboken, NJ, USA. doi:10.1002/9781118156247.ch20.
2. **Nordholt N, Kanaris O, Schmidt SBI, Schreiber F**. 11 2021. Persistence against benzalkonium chloride promotes rapid evolution of tolerance during periodic disinfection. Nat Commun 12 (1):1–13. doi:10.1038/s41467-021-27019-8.
3. **Pedreira A, Taşkın Y, García MR**. 1 2021. A Critical Review of Disinfection Processes to Control SARS-CoV-2 Transmission in the Food Industry. Foods 10 (2):283. doi:10.3390/foods10020283.
4. **European Food Safety Authority (EFSA), Centers for Disease Control and Prevention (CDC)**. 2 2021. The European Union One Health 2019 Zoonoses Report. EFSA J 19 (2). doi:10.2903/j.efsa.2021.6406.
5. **Rodríguez-López P, Rodríguez-Herrera JJ, Vázquez-Sánchez D, Cabo ML**. 6 2018. Current knowledge on Listeria monocytogenes biofilms in Food-Related environments: Incidence, resistance to biocides, ecology and biocontrol. MDPI Multidisciplinary Digital Publishing Institute doi:10.3390/foods7060085.
6. **Saá Ibusquiza P, Herrera JJR, Vázquez-Sánchez D, Parada A, Cabo ML**. 10 2012. A new and efficient method to obtain benzalkonium chloride adapted cells of Listeria monocytogenes. J Microbiol Methods 91 (1):57–61. doi:10.1016/j.mimet.2012.07.009.
7. **Jiang X, Yu T, Liang Y, Ji S, Guo X, Ma J, Zhou L**. 1 2016. Efflux pump-mediated benzalkonium chloride resistance in Listeria monocytogenes isolated from retail food. Int J Food Microbiol 217:141–145. doi:10.1016/j.ijfoodmicro.2015.10.022.
8. **Rodríguez-López P, Puga CH, Orgaz B, Cabo ML**. 9 2017. Quan-

ms Submission Template mSystems Submission Template mSystems Submission Template mSystems Submission Template mSystems Submission Template mSystems Submission Template

tifying the combined effects of pronase and benzalkonium chloride in removing late-stage Listeria monocytogenes–Escherichia coli dual-species biofilms. Biofouling 33 (8):690–702. doi:10.1080/08927014.2017.1356290.

9. **Romanova NA, Wolffs PFG, Brovko LY, Griffiths MW**. 5 2006. Role of Efflux Pumps in Adaptation and Resistance of Listeria monocytogenes to Benzalkonium Chloride. Appl Environ Microbiol 72 (5):3498–3503. doi:10.1128/AEM.72.5.3498-3503.2006.
10. **Guérin A, Bridier A, Le Grandois P, Sévellec Y, Palma F, Félix B, Roussel S, Soumet C**. 2 2021. Exposure to Quaternary Ammonium Compounds Selects Resistance to Ciprofloxacin in Listeria monocytogenes. Pathogens 10 (2):220. doi:10.3390/pathogens10020220.
11. **Chmielowska C, Korsak D, Szuplewska M, Grzelecka M, Maćkiw E, Stasiak M, Macion A, Skowron K, Bartosik D**. 9 2021. Benzalkonium chloride and heavy metal resistance profiles of Listeria monocytogenes strains isolated from fish, fish products and food-producing factories in Poland. Food Microbiol 98:103756. doi:10.1016/j.fm.2021.103756.
12. **To MS, Favrin S, Romanova N, Griffiths MW**. 11 2002. Postadaptational resistance to benzalkonium chloride and subsequent physicochemical modifications of Listeria monocytogenes. Appl Environ Microbiol 68 (11):5258–5264. doi:10.1128/AEM.68.11.5258-5264.2002/FORMAT/EPUB.
13. **Mereghetti L, Quentin R, Marquet-Van Der Mee N, Audurier A**. 11 2000. Low sensitivity of Listeria monocytogenes to quaternary ammonium compounds. Appl Environ Microbiol 66 (11):5083–5086. doi:10.1128/AEM.66.11.5083-5086.2000.
14. **Duze ST, Marimani M, Patel M**. 2021. Tolerance of Listeria monocytogenes to biocides used in food processing environments. Food Microbiol 97 (February):103758. doi:10.1016/j.fm.2021.103758.
15. **Alkhalifa S, Jennings MC, Granata D, Klein M, Wuest WM, Minbiole KPC, Carnevale V**. 5 2020. Analysis of the Destabilization of Bacterial Membranes by Quaternary Ammonium Compounds: A Combined Experimental and Computational Study. ChemBioChem 21 (10):1510–1516. doi:10.1002/cbic.201900698.
16. **Gyürék LL, Finch GR**. 9 1998. Modeling Water Treatment Chemical Disinfection Kinetics. J Environ Eng 124 (9):783–793. doi:10.1061/(asce)0733-9372(1998)124:9(783).
17. **Mouton JW, Vinks AA**. 2005. Pharmacokinetic/pharmacodynamic modelling of antibacterials in vitro and in vivo using bacterial growth and kill kinetics: The minimum inhibitory concentration versus stationary concentration. Clin Pharmacokinet 44 (2):201–210. doi:10.2165/00003088-200544020-00005.
18. **Pedreira A, Vázquez JA, García MR**. 2022. Kinetics of bacterial adaptation, growth and death at didecyldimethylammonium chloride sub-MIC concentrations. Front Microbiol 13:758237. doi:10.3389/fmicb.2022.758237.
19. **Chen Y, Geurts M, Sjollema SB, Kramer NI, Hermens JLM, Droge STJ**. 3 2014. Acute toxicity of the cationic surfactant C12-benzalkonium in different bioassays: How test design affects bioavailability and effect concentrations. Environ Toxicol Chem 33 (3):606–615. doi:10.1002/etc.2465.
20. **García MR, Cabo ML**. 2018. Optimization of E. coli inactivation by benzalkonium chloride reveals the importance of quantifying the inoculum effect on chemical disinfection. Front Microbiol 9 (JUN). doi:10.3389/fmicb.2018.01259.
21. **Harris LK, Theriot JA**. 6 2016. Relative Rates of Surface and Volume Synthesis Set Bacterial Cell Size. Cell 165 (6):1479–1492. doi:10.1016/J.CELL.2016.05.045.
22. **Chis OT, Villaverde AF, Banga JR, Balsa-Canto E**. 12 2016. On the relationship between sloppiness and identifiability. Math Biosci 282:147–161. doi:10.1016/j.mbs.2016.10.009.
23. **Salton MRJ**. 7 1968. Lytic Agents, Cell Permeability, and Monolayer Penetrability The Journal of General Physiology. The J Gen Physiol 52 (1):227–252. http://www.ncbi.nlm.nih.gov/pubmed/19873623http://www.pubmedcentral.nih.gov/articlerender.fcgi?artid=PMC2225791.
24. **Denyer SP, Stewart GSAB**. 4 1998. Mechanisms of action of disinfectants. Int Biodeterior Biodegrad 41 (3-4):261–268. doi:10.1016/S0964-8305(98)00023-7.
25. **Russell AD**. 1990. Mechanisms of Bacterial Resistance to Biocides.
26. **Mcdonnell G, Russell AD**. 1999. Antiseptics and disinfectants: Activity, action, and resistance. Clin Microbiol Rev 12 (1):147–179. doi:10.1128/cmr.12.1.147.
27. **Maillard JY**. 5 2002. Bacterial target sites for biocide action. J Appl Microbiol Symp Suppl 92 (1):16S–27S. doi:10.1046/j.1365-2672.92.5s1.3.x.
28. **Minbiole KPC, Jennings MC, Ator LE, Black JW, Grenier MC, LaDow JE, Caran KL, Seifert K, Wuest WM**. 6 2016. From antimicrobial activity to mechanism of resistance: the multifaceted role of simple quaternary ammonium compounds in bacterial eradication. Tetrahedron 72 (25):3559–3566. doi:10.1016/j.tet.2016.01.014.
29. **Morrison KR, Allen RA, Minbiole KPC, Wuest WM**. 9 2019. More QACs, more questions: Recent advances in structure activity relationships and hurdles in understanding resistance mechanisms. Tetrahedron Lett 60 (37):150935. doi:10.1016/j.tetlet.2019.07.026.
30. **Carey AB, Ashenden A, Köper I**. 3 2022. Model architectures for bacterial membranes. Biophys Rev 2022 14:1 14 (1):111–143. doi:10.1007/S12551-021-00913-7.
31. **Zhao W, Gurtovenko AA, Vattulainen I, Karttunen M**. 2012. Cationic Dimyristoylphosphatidylcholine and Dioleoyloxytrimethylammonium Propane Lipid Bilayers: Atomistic Insight for Structure and Dynamics. J. Phys. Chem. B 116:269–276. doi:10.1021/jp210619q.
32. **Nielsen EI, Khan DD, Cao S, Lustig U, Hughes D, Andersson DI, Friberg LE**. 11 2017. Can a pharmacokinetic/pharmacodynamic (PKPD) model be predictive across bacterial densities and strains? External evaluation of a PKPD model describing longitudinal in vitro data. J Antimicrob Chemother 72 (11):3108–3116. doi:10.1093/jac/dkx269.
33. **Kovacevic J, Wałecka-Zacharska E, Kitts DD, Ziegler J, Gilmour MW, Wałecka-Zacharska E, Reimer A, Gilmour MW**. 2016. Tolerance of Listeria monocytogenes to Quaternary Ammonium Sanitizers Is Mediated by a Novel Efflux Pump Encoded by emrE. Appl Environ Microbiol 82 (3):939–953. doi:10.1128/AEM.3741-15.
34. **Rakic-Martinez M, Drevets DA, Dutta V, Katic V, Kathariou S**. 2011. Listeria monocytogenes Strains Selected on Ciprofloxacin or the Disinfectant Benzalkonium Chloride Exhibit Reduced Susceptibility to Ciprofloxacin, Gentamicin, Benzalkonium Chloride, and Other Toxic Compounds. APPLIED AND ENVIRONMENTAL MICROBIOLOGY 77 (24):8714–8721. doi:10.1128/AEM.05941-11.
35. **Gilbert P, Moore LE**. 10 2005. Cationic antiseptics: Diversity of action under a common epithet. J Appl Microbiol 99 (4):703–715. doi:10.1111/j.1365-2672.2005.02664.x.
36. **Rodríguez-López P, Bernárdez M, Rodríguez-Herrera JJ, Comesaña AS, Cabo ML**. 1 2019. Identification and metagenetic characterisation of Listeria monocytogenes-harbouring communities present in food-related industrial environments. Food Control 95 (July 2018):6–17. doi:10.1016/j.foodcont.2018.07.023.
37. **Dare K, Shepherd J, Roy H, Seveau S, Ibba M**. 5 2014. LysPGS formation in Listeria monocytogenes has broad roles in maintaining membrane integrity beyond antimicrobial peptide resistance. Virulence 5 (4):534–546. doi:10.4161/viru.28359.
38. **Fischer W, Leopold K**. 1999. Polar lipids of four listeria species

containing L-lysylcardiolipin, a novel lipid structure, and other unique phospholipids. Int J Syst Bacteriol 49 (2):653–662. doi: 10.1099/00207713-49-2-653.

39. **Van Der Spoel D, Lindahl E, Hess B, Groenhof G, Mark AE, Berendsen HJC**. 2005. GROMACS: Fast, flexible, and free. J Comput Chem 26 (16):1701–1718.
40. **Lee J, Cheng X, Swails JM, Yeom MS, Eastman PK, Lemkul JA, Wei S, Buckner J, Jeong JC, Qi Y, Jo S, Pande VS, Case DA, Brooks CL, MacKerell AD, Klauda JB, Im W**. 2016. CHARMM-GUI Input Generator for NAMD, GROMACS, AMBER, OpenMM, and CHARMM/OpenMM Simulations Using the CHARMM36 Additive Force Field. J Chem Theory Comput 12 (1):405–413. doi:10.1021/acs.jctc.5b00935.
41. **Jo S, Kim T, Iyer VG, Im W**. 2008. CHARMM-GUI: A web-based graphical user interface for CHARMM. J Comput Chem 29 (11):1859–1865. doi:10.1002/jcc.20945.
42. **Brooks BR, Brooks CL, Mackerell AD, Nilsson L, Petrella RJ, Roux B, Won Y, Archontis G, Bartels C, Boresch S, Caflisch A, Caves L, Cui Q, Dinner AR, Feig M, Fischer S, Gao J, Hodoscek M, Im W, Kuczera K, Lazaridis T, Ma J, Ovchinnikov V, Paci E, Pastor RW, Post CB, Pu JZ, Schaefer M, Tidor B, Venable RM, Woodcock HL, Wu X, Yang W, York DM, Karplus M**. 2009. CHARMM: The biomolecular simulation program. J Comput Chem 30 (10):1545–1614. doi:10.1002/jcc.21287.
43. **Wu EL, Cheng X, Jo S, Rui H, Song KC, Dávila-Contreras EM, Qi Y, Lee J, Monje-Galvan V, Venable RM, Klauda JB, Im W**. 2014. CHARMM-GUI Membrane Builder toward realistic biological membrane simulations. J Comput Chem 35 (27):1997–2004. doi: 10.1002/jcc.23702.
44. **Kim S, Lee J, Jo S, Brooks CL, Lee HS, Im W**. 2017. CHARMM-GUI ligand reader and modeler for CHARMM force field generation of small molecules. J Comput Chem 38 (21):1879–1886. doi:10.1002/jcc.24829.
45. **Humphrey W, Dalke A, Schulten K**. 1996. VMD: Visual molecular dynamics. J Mol Graph 14 (1):33–38. doi:10.1016/0263-7855(96)00018-5.
46. **Nosé S, Klein ML**. 1983. Constant pressure molecular dynamics for molecular systems. Mol Phys 50 (5):1055–1076. doi: 10.1080/00268978300102851.
47. **Parrinello M, Rahman A**. 1981. Polymorphic transitions in single crystals: A new molecular dynamics method. J Appl Phys 52 (12):7182–7190. doi:10.1063/1.328693.
48. **Balsa-Canto E, Henriques D, Gábor A, Banga JR**. 11 2016. AMIGO2, a toolbox for dynamic modeling, optimization and control in systems biology. Bioinformatics 32 (21):3357–3359. doi: 10.1093/bioinformatics/btw411.
49. **Vilas C, Arias-Méndez A, García MR, Alonso AA, Balsa-Canto E**. 2018. Toward predictive food process models: A protocol for parameter estimation. Crit Rev Food Sci Nutr 58 (3):436–449. doi: 10.1080/10408398.2016.1186591.
50. **García MR**. 6 2022. Model&Data of L. monocyotegenes inactivation (time-kill curves) with Benzalkonium chloride (BAC). Zenodo doi: 10.5281/ZENODO.6651604.

mSystems Submission Template mSystems Submission Template mSystems Submission Template mSystems Submission Template mSystems Submission Template mSystems Submission Template